Transition Met Chem (2013) 38:811–819
DOI 10.1007/s11243-013-9753-1

Synthesis, characterization, DNA-binding, photocleavage, cytotoxicity and docking studies of Co(III) mixed ligand complexes

Yata Praveen Kumar · C. Shobha Devi · N. Deepika · Nazar MD Gabra · Nishant Jain · A. Srishailam · Kotha Laxma Reddy · S. Satyanarayana

Received: 28 May 2013 / Accepted: 1 August 2013 / Published online: 21 August 2013

Abstract A new ligand, (2-ethoxy-6-(1H imadazo[4,5-f][1,10]phenanthroline-2-yl)phenol) (HEPIP) and its three Co(III) complexes $[Co(phen)_2(HEPIP)](ClO_4)_3$ (**1**), $[Co(bpy)_2(HEPIP)](ClO_4)_3$ (**2**) and $[Co(dmb)_2(HEPIP)](ClO_4)_3$ (**3**) have been synthesized and characterized. All three Co(III) complexes exhibited antitumor activity against four human tumor cell lines. The interaction of these complexes with calf thymus DNA was studied by absorption and emission spectroscopy, viscosity measurements and DNA cleavage assays. The DNA-binding constants of complexes **1**, **2** and **3** were determined as 6.13×10^5, 4.46×10^5 and 3.72×10^5 M^{-1}, respectively. The complexes appear to interact with DNA through intercalation. Studies on the mechanism of photocleavage indicated that both superoxide anion radical and singlet oxygen may play an important role.

Introduction

Metal complexes that can bind to DNA are gaining considerable attention owing to their diverse applications as diagnostic agents for medical applications, cleavage agents for probing nucleic acid structure [1, 2] and identifiers of transcription start sites [3]. Small molecules can bind to DNA by different mechanisms, and binding studies are important for the design of new and more efficient drugs targeted to DNA [4]. Small molecules typically bind to DNA by non-covalent interactions such as electrostatic binding, groove binding and intercalative binding. Intercalating and groove binding molecules are important tools in molecular biology, and many are clinically useful in the treatment of cancer [5, 6]. Intercalation behavior is often related to the antitumor activity of the compound [7, 8].

Cisplatin and its analogs are widely used as antitumor drugs [9]. The search for new metallo-anticancer drugs, which drives much current research [10], currently includes a focus on ruthenium complexes. Octahedral complexes with a dipyridophenazine ligand have been much studied, because of the "Light switch effect" [11]. The crystal structure of $[Ru(phen)_2DPPZ]^{2+}$ (DPPZ = dipyrido[3,2-*a*:2′,3′-*c*] phenazine) with an oligonucleotide was reported by Niyazi et al. [12].

There have been intensive efforts to investigate factors that determine affinity and selectivity in the binding of small molecules to DNA [13], since information about these factors would be valuable for the design of sequence-specific DNA-binding molecules for applications in chemotherapy and in the development of tools for biotechnology [14]. In our group, much effort has been devoted to studying the DNA interactions and cytotoxicities of novel polypyridyl complexes containing different intercalative ligands [15–19].

In this article, we report three Co(III) mixed ligand polypyridyl complexes, $[Co(phen)_2HEPIP](ClO_4)_3$ (**1**), $[Co(bpy)_2HEPIP](ClO_4)_3$ (**2**) and $[Co(dmb)_2HEPIP](ClO_4)_3$ (**3**), their DNA-binding behavior, and their abilities to

Electronic supplementary material The online version of this article (doi:10.1007/s11243-013-9753-1) contains supplementary material, which is available to authorized users.

Y. P. Kumar · C. S. Devi · N. Deepika · N. M. Gabra · A. Srishailam · K. L. Reddy · S. Satyanarayana (✉)
Department of Chemistry, Osmania University, Hyderabad 500007, Andhra Pradesh, India
e-mail: ssnsirasani@gmail.com

N. Jain
Chemical Biology Division, Indian Institute of Chemical Technology, Hyderabad 50060, Andhra Pradesh, India

induce cleavage of pBR322 DNA. Cell viability experiments indicated that the Co(III) complexes showed significant dose-dependent cytotoxicities against four human tumor cell lines, namely, human cervical cancer (HeLa), human alveolar adenocarcinoma (A549), prostate cancer (DU145) and hepatocellular carcinoma (HEPG). The complexes were also tested for antimicrobial activity and docked into DNA base pairs using a docking program [20, 21].

Experimental

Materials and methods

$CoCl_2 \cdot 6H_2O$, 1,10-phenanthroline monohydrate, 2,2′-bipyridine and 4,4′-dimethyl-2,2′-bipyridine were purchased from Merck. CT-DNA and supercoiled (CsCl purified) pBR322 DNA (Bangalore Genei, India) were used as received. All other common chemicals and solvents were procured from locally available sources; solvents were purified before use by standard procedures [22]. Deionized, double-distilled water was used for preparing various buffers. Solutions of DNA in 5 mM Tris-HCl buffer (pH = 7.2) and 50 mM NaCl gave a ratio of UV absorbance at 260 and 280 nm of about 1.8–1.9:1, indicating that the DNA was sufficiently free of protein [23]. The concentration of CT-DNA was determined spectrophotometrically using the molar absorption coefficient 6,600 M^{-1} cm^{-1} (260 nm) [24]. Human tumor cell lines were obtained from NCCS, Pune, and maintained in RPMI 1640 medium (Sigma Aldrich) supplemented with 10 % fetal bovine serum, 1 % penicillin, and streptomycin in a humidified 5 % CO_2 atmosphere.

Synthesis and characterization

1,10-Phenanthroline-5,6-dione [25], cis-$[Co(phen)_2Br_2]$-$Br \cdot 2H_2O$, cis-$[Co(bpy)_2Br_2]Br \cdot 2H_2O$ and cis-$[Co(bpy)_2Br_2]$-$Br \cdot 2H_2O$ [26, 27] were prepared according to the methods used in our previous study and the literature, respectively [28, 29]. The syntheses of the free ligands and their Co(III) complexes are shown in Scheme 1.

Synthesis of HEPIP

A solution of 1,10-phenanthroline-5,6-dione (0.25 g, 1.2 mmol), 3-ethoxy salicylaldehyde(0.31 g, 1.9 mmol)

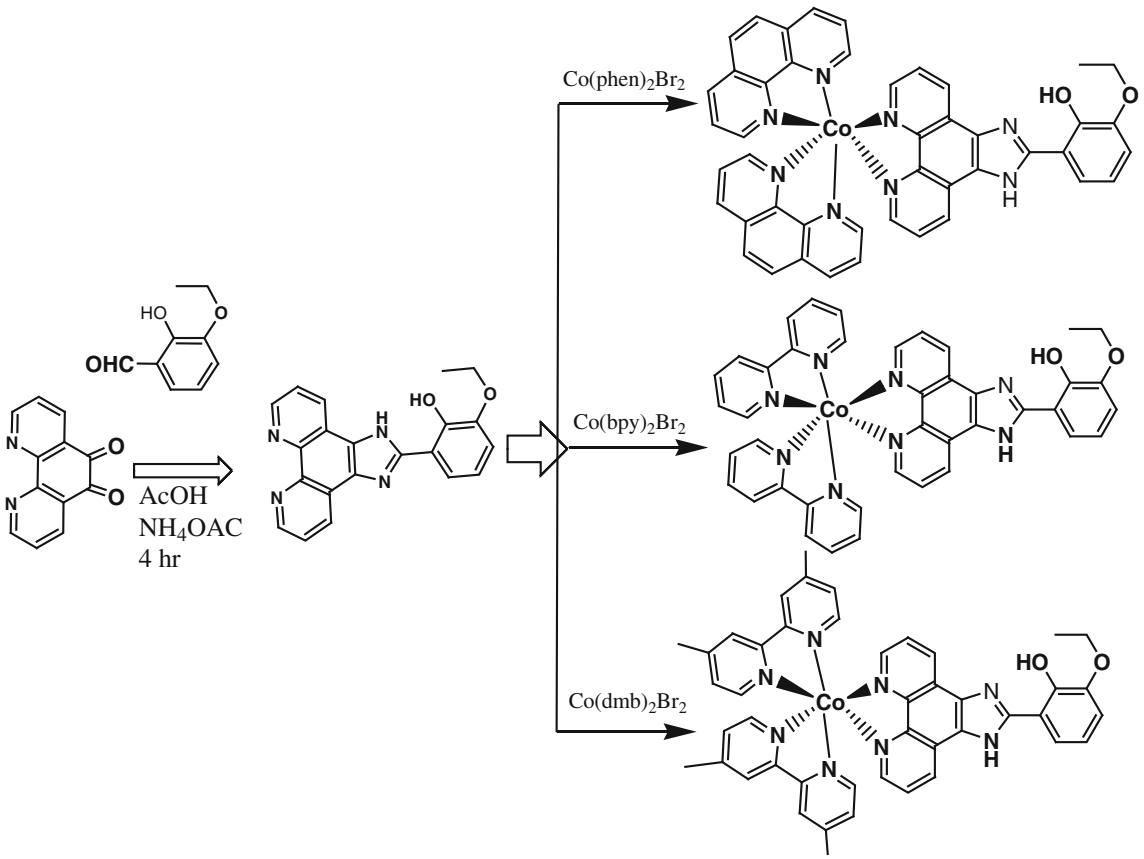

Scheme 1 Synthetic routes of ligand and Co(III) complexes

and ammonium acetate (1.9 g, 25 mmol) in glacial acetic acid (10 mL) was refluxed for 4 h. The light yellow solution so obtained was cooled, diluted with water (25 cm^3) and neutralized with ammonia. The precipitate was filtered off, washed with H_2O and Me_2CO and then dried. Yield: 0.75 g (72 %).

ESI–MS (in DMSO), m/z; 358 (Calcd 357);Calcd for $C_{21}H_{16}N_4O_2$ %: C, 70.5; H, 4.7; N, 15.6; Found (%); C, 70.1; H, 4.4; N, 15.2. IR (KBr cm^{-1}): 1,655 (C=N), 1,510 (C=C). ^{1}HNMR (DMSO-d6, 25 °C, δ ppm, J = Hz); 9.1 (1Hs); 9.0 (2H, d, $J = 7.2$); 8.9 (2H, d 7.6); 6.5–7.8 (1H, m); 7.1 (1H,d $J = 6.9$); 6.8–7.2 (1H, m) 6.9 (1H, d, $J = 7.5$); 5.8 (^{1}H, N H, s); 3.2 (2H,q),1.4 (3H,t); ^{13}C[^{1}H]-NMR (DMSO-d_6, δ ppm): 150, 148, 145, 139, 135, 132, 130, 125, 124, 116, 115, 113, 110, 65 and 16.

Synthesis of complex **1**

A mixture of cis-[$Co(phen)_2Br_2$]$Br{\cdot}2H_2O$ (0.57 g, 1.0 mmol) and HEPIP (0.48 g, 1.5 mmol) in EtOH (50 cm^3) was refluxed for 4 h to give a yellow solution. After filtration, the complex was precipitated by addition of a saturated ethanolic solution of $NaClO_4$. The complex was filtered off and dried under vacuum before recrystallization (Me_2CO–Et_2O). Yield: (79 %). $C_{45}H_{32}Cl_3CoN_8O_{14}$; Calcd (%); C, 48.9; H, 3.1; N, 10.4. Found (%): C, 49.1; H, 3.4; N, 10.2. IR (KBr cm^{-1}): ESI–MS (in DMSO), m/z; 1,073 (Calcd 1,072). 1,424 (C=N), 1,337 (C=C), 625 (Co–N(HEPIP)), 456 (Co–N(phen)). ^{1}H-NMR (DMSO-d_6, 25 °C, δ ppm, J = Hz): 9.1 (2H s); 9.0 (2H,d, $J = 7.8$); 8.9 (2H, d, $J = 6.8$); 6.7–7.9 (1H, m); 7.1 (1H,d, $J = 6.8$);6.9–7.6 (1H, m) 6.9 (1H, d, $J = 7.7$); 5.7 (^{1}H, NH,); 3.5–4.2 (2H,q),1.6–2.1 (3H,t);^{13}C[^{1}H]-NMR (DMSO-d_6, δ ppm): 151, 149.5, 146, 143, 138, 135, 131, 128, 129, 117, 116, 112, 110, 66.5 and 20.

Synthesis of complex **2**

This complex was obtained by a procedure similar to that described above, except that [$Co(bpy)_2Br_2$]$Br{\cdot}2H_2O$ (0.53 g, 1.0 mmol) was used in place of cis-[$Co(phen)_2Br_2$]-$Br{\cdot}2H_2O$. (Yield: 72 %). $C_{41}H_{32}Cl_3CoN_8O_{14}$; Calcd (%): C, 46.5; H, 3.2; N, 10.8. Found (%): C, 46.2; H, 3.1; N, 11.1. ESI–MS (in DMSO), m/z; 1,025 (Calcd 1,024). IR (KBr cm^{-1}): 1,466 (C=N), 1,374 (C=C), 627 (Co–N (HEPIP)), 476 (Co–N(bpy)).^{1}H-NMR (DMSO-d_6, 25 °C, δ ppm, J = Hz): 9.4 (2H s); 9.1 (2H,d, $J = 7.6$); 8.6 (2H, d, $J = 6.9$); 7.5–7.9 (1H, m); 7.0 (1H, d); 6.8–7.2 (1H, m) 6.6 (1H, d, $J = 7.3$); 5.68 (1H, NH, s); 3.4–3.8 (2H, q),1.6–1.9 (3H, t); ^{13}C[^{1}H]-NMR (DMSO-d_6, δ ppm): 152, 155, 146, 143, 138, 134, 131, 127, 128, 117, 115, 112, 110, 66 and 18.

Synthesis of complex **3**

This complex was obtained by a procedure similar to that described above, but using cis-[$Co(dmb)_2Br_2$]$Br{\cdot}2H_2O$(0.587 g, 1.0 mmol) in place of cis-[$Co(phen)_2Br_2$]-$Br{\cdot}2H_2O$. Yield: (65 %). $C_{45}H_{40}Cl_3CoN_8O_{14}$; Calcd (%): C, 49.4; H, 3.8; N, 10.5. Found (%): C, 48.9; H, 3.2; N, 10.8. ESI–MS (in DMSO), m/z; 1,082 (Calcd 1,080). IR (KBr cm^{-1}): 1,438 (C=N), 1,307 (C=C), 629 (Co–N(HEPIP)), 485 (Co–N(dmb)); UV–Vis (CH_3OH λmax, nm (log ε): 261 (3.60), 271 (3.58), 429 (3.28);^{1}H-NMR (DMSO-d_6, 25 °C, δ ppm, J = Hz): 9.1 (2H, s); 9.1 (2H,d, $J = 6.8$); 8.5 (2H, d, $J = 7.2$); 7.5–8.8 (1H, m); 7.1 (1H, d, $J = 7.2$);6.8–7.4 (1H, m) 6.9 (1H, d, $J = 6.6$); 5.80 (1H, NH, s); 3.2–3.8 (2H, q), 2.2–2.9 (3H, t), 2.1 (4 methyl); ^{13}C[^{1}H]-NMR (DMSO-d_6, δ ppm): 153, 150, 146, 143, 138, 134, 131, 127, 128, 117, 114, 112, 109, 67 and 20.

Physical measurements

UV–Visible spectra were recorded with an Elico Bio-spectrophotometer, model BL198. IR spectra were recorded in KBr discs on a Perkin-Elmer FT-IR-1605 spectrometer. ^{1}H and ^{13}C [^{1}H]NMR spectra were measured on a Bruker Z-Gradient single axis fitted with a high-resolution probe and 400 MHz standard spectrometer using DMSO-d_6 as the solvent and TMS as an internal standard. Microanalysis was performed on a Perkin-Elmer 240 elemental analyzer. Fluorescence spectra were recorded with an Elico spectrofluorimeter model SL 174.

The DNA-binding experiments were performed in Tris–HCl buffer at 25 °C. The absorption titrations were performed at a fixed complex concentration, to which the DNA stock solution was gradually added up to the point of saturation. The mixture was allowed to equilibrate for 5 min before the spectra were recorded. The emission intensities were recorded in the range of 520–720 nm. In these emission studies, fixed complex concentrations (10 μM) were taken and to this, varying concentrations (0–100 μM) of DNA were added. The excitation wavelength was fixed, and the emission range was adjusted before measurements. The fraction of the ligand bound was calculated from the relation,

$$C_b = C_t[(F - F_0)/(F_{max} - F_0)]$$

where C_t is the total complex concentration, F is the observed fluorescence emission intensity at a given DNA concentration, F_0 is the intensity in the absence of DNA and F_{max} is when the complex is fully bound to DNA. The binding constant (K_b) was obtained from a modified Scatchard equation [30], from a Scatchard plot of r/C_f versus r, where r is C_b/[DNA] and C_f is the concentration of free complex.

Viscosity experiments were carried out with an Ostwald viscometer. DNA samples approximately 200 base pairs in average length were prepared by sonication in order to minimize complexities arising from DNA flexibility [31]. Data were analyzed as $(\eta/\eta^{\circ})^{1/3}$ versus [Co]/[DNA], where η is viscosity of DNA in the presence of complex and η° is the viscosity of DNA alone. Viscosity values were calculated from the observed flow time of DNA-containing solutions ($t > 100$ s) corrected for the flow time of buffer alone (t°), $\eta = t - t_0$ [32].

For gel electrophoresis experiments, supercoiled pBR322 DNA (100 μM) was treated with the appropriate complex in 50 mM Tris–HCl and 18 mM NaCl buffer pH 7.8, and the solutions were then irradiated at room temperature with a UV lamp (10 W). The samples were analyzed by electrophoresis for 2.5 h at 40 V on a 1 % agarose gel in Tris–acetic acid–EDTA buffer, pH 7.2. The gels were stained with 1 mg mL^{-1}ethidium bromide and photographed under UV light.

Antimicrobial tests were performed by the standard disc diffusion method [33]. The complexes were screened for antifungal activity against *Aspergillus niger* and *Fusarium oxysporium*, which were isolated from the infected parts of host plants grown on *M* test agar medium. The cultures of the fungi were purified by single-spore isolation technique. A concentration of 1.5 mg mL^{-1} of each cobalt complex in DMSO was prepared for testing against spore germination of each fungus. Filter paper discs of 5 mm were prepared using Whatman filter paper no. 1 (sterilized in an autoclave) and saturated with 10 mL of the cobalt complex dissolved in DMSO. The fungal culture plates were inoculated and incubated at 25 ± 2 °C for 48 h. The plates were then observed, and the diameters of the inhibition zones (in millimeters) were measured and tabulated. The results were also compared with the standard antifungal drug fluconazole at the same concentration. The antibacterial activities of the complexes were studied against *Staphylococcus aureus* (MTCC 96) and *Escherichia coli* (MTCC 443). Each complex was dissolved in DMSO at 1 mg mL^{-1}. Paper discs of Whatman filter paper no. 1 were cut and sterilized in an autoclave. The paper discs were saturated with 10 mL of the cobalt complex dissolved in DMSO or DMSO as negative control and placed aseptically in Petri dishes containing *M* test agar media inoculated with *S. aureus or E. coli*. The Petri dishes were incubated at 37 °C, and the inhibition zones were recorded after 24 h. The experiments were repeated, and the average of the two runs was taken. The results were also compared with the standard antibacterial drug streptomycin at the same concentration.

The MTT (MTT = 3-(4,5-dimethylthiazol-2-yl)-2,5-diphenyltetrazolium bromide) assay was used [34] to determine the viability of tumor cells; upon treatment with complexes **1–3,** cells were placed in 96-well micro-assay culture plates (8×10^3 cells per well) and grown overnight at 37 °C in a 5 % CO_2 incubator. The test complexes were dissolved in DMSO and diluted with RPMI 1640 (RPMI = Roswell Park Memorial Institute medium) and then added to the wells to achieve final concentrations ranging from 10 to 100 μM. After treatment of tumor cells with the complexes for 48 h, the plates were washed twice with culture medium, then MTT was added and the plates were incubated for another 4 h. Cells without added Co(III) complexes were used as negative control. Cisplatin was used as the positive control. The IC_{50} values were determined by plotting the percentage viability versus concentration on a logarithmic graph and reading of the concentration at which 50 % of cells remained viable relative to the control. Each experiment was repeated at least three times to obtain mean values.

The molecular docking calculations on all three complexes were done using the 3.01 GOLD (Genetic Optimization for Ligand Docking) program 55, which is based on Genetic Algorithms. This method allows partial flexibility of the hydroxyl groups of the respective DNA molecule and full flexibility of the ligand. The DNA sequences used for the docking simulations were obtained from the Protein Data Bank and are double helices associated with ligands. Using Discovery Studio 3.0, we built the DNA sequence (CGATTAATCG) obtained from the Protein Data Bank (PDB: 1D49) double helix DNA decamer. The DNA structures were chosen so as to allow an evaluation of the binding preference for CG sequences. In order to evaluate the GOLD scoring function, all water molecules were removed from the DNA molecules. The function fitted was Gold Score. Hypothetical structures resulting from the initial docking were energy-minimized. The docking procedure depended on two principal features: (1) an energy (or scoring) function for evaluating trial configurations of the two interacting molecules and (2) an algorithm for seeking the best achievable minimum of this function. The two interacting molecules were considered as rigid bodies, and the sum of the van der Waals, hydrogen bonding and electrostatic energy terms were used as the scoring function.

Results and discussion

Characterization

The ESI–MS spectrum of HEPIP shows a molecular ion peak at m/z 358, equivalent to its molecular weight (Calcd 357). The ^{1}H-NMR spectrum of HEPIP gave a peak at 9.1 (singlet) corresponding to OH, a quartet at 3.2 and triplet at 1.4 ppm corresponding to CH_2 and CH_3 protons and a broad peak at 5.8 (singlet) corresponding to –NH. The

remaining signals belong to the ring protons between 9.0 and 6.9 ppm and were observed with proper multiplicity. The protons next to nitrogen appeared downfield as a doublet at 9.0 ppm. The ^{13}CNMR spectrum of HEPIP gave a peak at 148 ppm corresponding to COH carbon, 145 corresponding to carbon next to nitrogen and the ethoxy carbon at 65 ppm, and 16(methyl) other peaks were observed in the aromatic region as expected.

The ESI–MS spectrum of $[Co(phen)_2(HEPIP)](ClO_4)_3 \cdot 2H_2O$ showed the molecular ion peak at m/z of 1,073 (Calcd 1,072). The IR spectrum of this complex showed bands at 1,424 (C=N) and 1,337 (C=C), shifted to a lower frequency when compared to free ligand consistent with complexation. New bands at 625 and 456 cm^{-1} assigned to Co–N (HEPIP) and Co–N(phen), respectively, support complex formation. In the ^{1}HNMR spectrum peaks due to the various protons of phen and HEPIP are shifted downfield upon complexation. The ^{13}CNMR spectrum showed that the carbon next to nitrogen shifted downfield to 146 ppm. The carbon attached to OH was shifted downfield to 151, and ethoxy and methyl carbons resonate at 66 and 20 ppm, respectively. Aromatic peaks are also shifted downfield. The ESI–MS spectrum of $[Co(bpy)_2(HEPIP)](ClO_4)_3 \cdot 2H_2O$ shows a molecular ion peak at m/z of 1,032 which is equivalent to its molecular weight (Calcd 1,031). The IR spectrum of this complex includes bands at 1,466 (C=N) and 1,374 (C=C), which are shifted to lower frequency when compared to the free ligand, indicating complexation. New bands at 630 and 580 cm^{-1} assigned to Co–N(HEPIP) and Co–N(bpy), respectively, support complex formation. The ^{1}HNMR spectrum of $[Co(bpy)_2(HEPIP)](ClO_4)_3 \cdot 2H_2O$ shows the various protons of bpy and HEPIP are shifted downfield upon complexation. In the ^{13}CNMR spectrum of this complex, the signal at 152 ppm, which is next to nitrogen, is shifted downfield, while the carbon attached to OH is shifted downfield to 150 ppm and the ethoxy carbon resonates at 66 ppm. Peaks in the aromatic region are also shifted downfield.

The ESI–MS spectrum of $[Co(dmb)_2(HEPIP)](ClO_4)_3 \cdot H_2O$ shows a molecular ion peak at m/z of 1,082 which is equivalent to its molecular weight (Calcd 1,080). In the ^{1}HNMR spectrum peaks due to various protons of the dmb and HEPIP ligands are shifted downfield upon complexation. In the ^{13}CNMR spectrum, the C next to nitrogen is shifted downfield to 153 ppm, while the carbon attached to OH shifts downfield to 156 ppm, and the ethoxy and methyl carbons resonate at 67 and 18 ppm respectively. The aromatic peak are also shifted downfield.

Electronic absorption

For metallo-intercalators, DNA binding is associated with hypochromism and a red shift in the MLCT and ligand bands [35]. The electronic spectra of these complexes in the absence and presence of CT-DNA are illustrated in Fig. 1, and the data are summarized in Table 1. Bands at λ_{max} 430 nm (**1**), 428 nm (**2**) and 425 nm (**3**) are assigned to MLCT [36], while the bands at λ_{max} 265 nm (**1**), 262 nm (**2**) and 263 nm (**3**) are due to π–π* transitions of HEPIP. Addition of increasing quantities of CT-DNA results in decreasing peak intensities. As the DNA concentration is increased, the MLCT bands of complexes **1**, **2** and **3** exhibit hypochromism of 20.6, 11.5 and 8.9 %, respectively, and bathochromism of about 3–6 nm. Intrinsic DNA-binding constants K were determined by monitoring the change of absorbance of the MLCT bands of the complexes with increasing concentration of DNA [37]. According to following equation [38],

$$[DNA]/(\varepsilon_a - \varepsilon_f) = [DNA]/(\varepsilon_b - \varepsilon_f) + 1/(K(\varepsilon_b - \varepsilon_f))$$

where [DNA] is the concentration of the base pairs, the apparent absorption coefficients ε_a, ε_f and ε_b correspond to A_{obsd}/[Co], the extinction coefficients for the free cobalt complex, the complex in the presence of DNA and the cobalt complex in the fully bound form, respectively. In plots of $[DNA]/(\varepsilon_a - \varepsilon_f)$ versus [DNA], K is given by the ratio of slope to intercept. The values of K so obtained were 6.13×10^5, 4.46×10^5 and 3.72×10^5 M^{-1}, for complex **1**, **2** and **3,** respectively. These spectroscopic characteristics suggest a stacking interaction between the complexes and the base pairs of DNA. The difference in binding strength of complexes **1** and **2** could be attributed to the different ancillary ligands; phenanthroline is more planar than bipyridyl; hence, the binding constant of complex **1** is higher than complex **2**. Similarly, the two additional

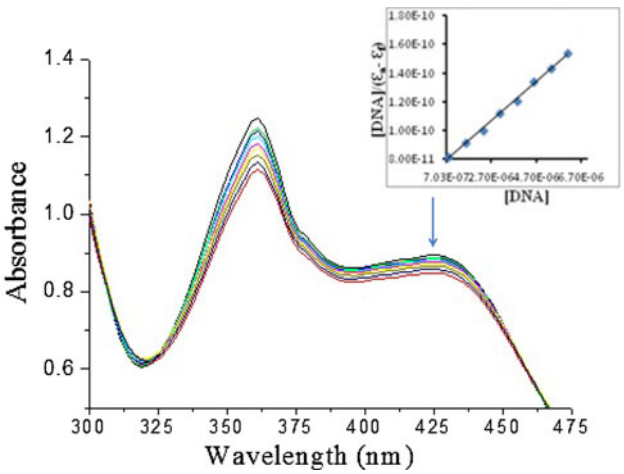

Fig. 1 Absorption spectrum of $[Co(bpy)_2 2\text{-HEPIP}]^{3+}$ (1) in Tris–HCl buffer at 25 °C in the presence of increasing amount of CT-DNA, [Co] = 10 mM, [DNA] = 0–120 mM. The *arrows* indicate the change in absorbance upon increasing the DNA concentration. Insert: Plot of $[DNA]/(\varepsilon_a - \varepsilon_f)$ versus [DNA] for titration of the Co(III) complexes

Table 1 Results of absorption titration experiments

Complexes	Hypochromicity (%)	Absorption λ_{max} (nm)		
		Free	Bound	$\Delta\lambda$
CT-DNA alone		–	–	–
$[Co(phen)_2$ 2-HEPIP$]^{3+}$	20.6	276	286	10
$[Co(bpy)_2$ 2-HEPIP$]^{3+}$	11.5	258	266	8
$[Co(dmb)_2$2-HEPIP$]^{3+}$	8.9	261	266	5

methyl groups of dimethyl bipyridyl in complex **3** exert steric hindrance; hence, complex **2** binds stronger than complex **3**. The HEPIP ligand contains a free hydroxy group, which may form intramolecular hydrogen bonds with the nitrogen of DNA.

Fluorescence spectroscopic studies

To further understand the nature of the complex binding to DNA, luminescence titration experiments were performed at a fixed metal complex concentration (5 μM) in Tris buffer (pH = 7.2) at ambient temperature. The change of emission intensity is related to the extent to which the complex enters into the hydrophobic environment within the DNA. Figure 2 shows the fluorescence excitation and emission spectra for the free and bound complexes in the presence of different amounts of CT-DNA. Excitation wavelengths of 433, 430 and 428 nm and emission wavelengths of 610, 618 and 627 nm for complexes **1**, **2** and **3,** respectively, were used for fluorescence measurements. Addition of DNA to a solution of each complex resulted in an increase in fluorescence intensity, by a factor of 1.54, 1.48 and 1.25 times, respectively. The intrinsic binding constant was obtained from the fluorescence data using a modified form of the Scatchard equation [30] with a plot of r/c_f versus r, where r is the binding ratio C_b/[DNA] and C_f is the free ligand concentration. These plots gave binding constants (K_b) of (5.45 ± 0.1) × 10^5 M^{-1}, (4.16 ± 0.1) × 10^5 M^{-1}, and (3.18 ± 0.1) × 10^5 M^{-1} for complexes **1**, **2** and **3,** respectively. The order of K_b values agrees with the results of the absorption studies.

Quenching studies

We next carried out emission quenching experiments using $[Fe(CN)_6]^{4-}$, which permits distinguishing of bound Co(III) species. Positively charged free complex ions should be readily quenched by $[Fe(CN)_6]^{4-}$,whereas when bound to DNA, the complex will be protected from the quencher because the highly negative charge of

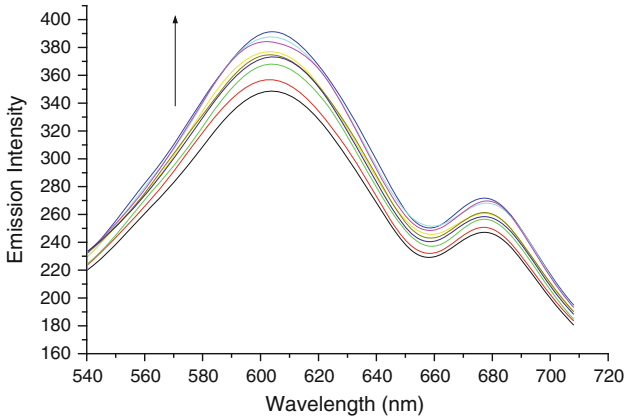

Fig. 2 Emission spectra of, $[Co(phen)_2$2-HEPIP$]^{3+}$ in Tris–HCl buffer at 25 °C upon addition of CT-DNA, [Co] = 20 μM, [DNA] = 0–120 μM. The *arrow* shows the increase in intensity upon increasing CT-DNA concentrations

$[Fe(CN)_6]^{4-}$ would be repelled by the negative DNA phosphate backbone. The method essentially consists of titrating a given amount of the DNA–metal complex with increasing concentrations of $[Fe(CN)_6]^{4-}$and measuring the change in fluorescence intensity (Fig. 3); in the absence of DNA, the complex is efficiently quenched by $[Fe(CN)_6]^{4-}$, resulting in linear Stern–Volmer plots. The Stern–Volmer quenching constant K_{sv} can be determined by using the Stern–Volmer equation [39];

$$I_0/I = 1 + K_{sv}[Q]$$

where I_0 and I are the fluorescence intensities in the absence and presence of the quencher, respectively, Q is the concentration of the quencher and K_{sv} is a linear Stern–Volmer quenching constant. Figure 3 shows the Stern–Volmer plots, which are linear for all three complexes [40, 41]. Ferrocyanide quenching curves for the three

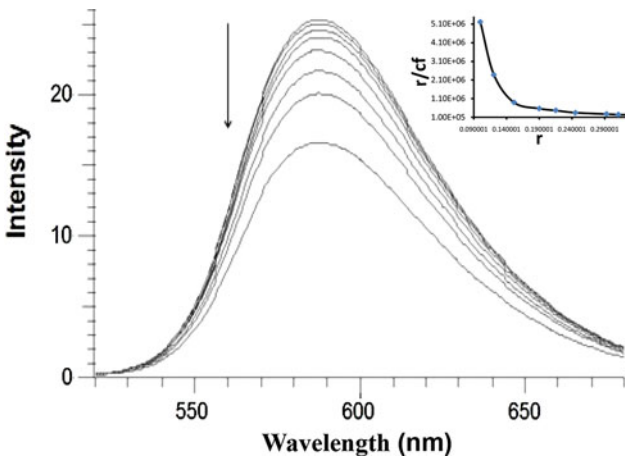

Fig. 3 Emission quenching of Co(III) complexes $[Co(phen)_2$2-HEPIP$]^{3+}$ with $K_4[Fe(CN)_6]^{4-}$ in the presence and absence of DNA. [Co] = 10 mM, [DNA]/[Co] = 40:1

complexes in the presence and absence of CT-DNA are shown in Fig. 3. The absorption, fluorescence and quenching studies all indicate that the binding constants are in the order **1** > **2** > **3**.

Viscosity studies

A hydrodynamic measurement such as viscosity is sensitive to DNA length change and is regarded as the least ambiguous and most critical test of a binding model. In classical intercalation, the DNA helix lengthens as base pairs are separated to accommodate the bound ligand, leading to an increase in the viscosity of the DNA solution [42, 43]. On the other hand, partial and/or nonclassical intercalation of the ligand may bind the DNA helix, resulting in a decrease in its effective length and concomitantly its viscosity. The effects of the three complexes on the viscosity of DNA are shown in Fig. 4. As the concentration of the complexes increases, the relative viscosity of DNA also increases, similar to the behavior of the proven DNA intercalator $[Ru(phen)_2dppz]^{2+}$ [44]. Although the intercalating ligand is the same in all three complexes, there are small differences in the viscosity, due to the difference in ancillary ligands. These results again suggest that these complexes show an intercalative binding mode to CT-DNA.

Photo-activated cleavage of pBR322 DNA

Plasmid pBR 322 DNA is mainly in the closed-circle supercoiled form (Form I). Intercalation of small molecules into plasmid DNA can cleave the supercoiled form, which decreases its mobility and can be visualized by gel electrophoresis; on the other hand, simple electrostatic interaction of small molecules with DNA does not significantly influence the supercoiled form; thus, the mobility of the supercoiled DNA does not change.

Plasmid pBR322 DNA was subjected to gel electrophoresis after incubation with the cobalt(III) complexes and irradiation at 365 nm. In control experiments where the complex was absent (lane 1) or the DNA-complex mixtures were incubated in the dark, no photocleavage was noticeable (Fig. 5). In contrast, irradiation with increasing concentrations of all three complexes (lanes 2–5) resulted in a decrease in the amount of supercoiled DNA, whereas the nicked (form II) increased, which is slow moving [45]. These results indicate that scission occurs on one strand (nicked). All three complexes are effective for photo-sensitized cleavage of DNA.

Antimicrobial activities

The antifungal activity data (Table 2) indicate that the complexes show appreciable activity *against A. niger and F. oxysporium* at 1.5 mg mL^{-1} concentration. The results for the compounds were compared with DMSO as control and are expressed as inhibition zone diameter (in millimeters) versus control. Complex **1** showed the highest activity against *A. niger* and moderate activity against *F. oxysporium*. This complex exhibited greater antifungal activity against *A. niger* compared to the standard drug fluconazole. Complexes **2** and **3** showed less activity than fluconazole. The antibacterial activity data (Table 3) indicate that the complexes have high activity against both *S. aureus* and *E. coli* at 1 mg mL^{-1} concentration. Complex **1** shows the highest activity (19 mm) against *S. aureus* and 18-mm inhibition against *E. coli*. This complex exhibits greater antibacterial activity against *S. aureus* than the

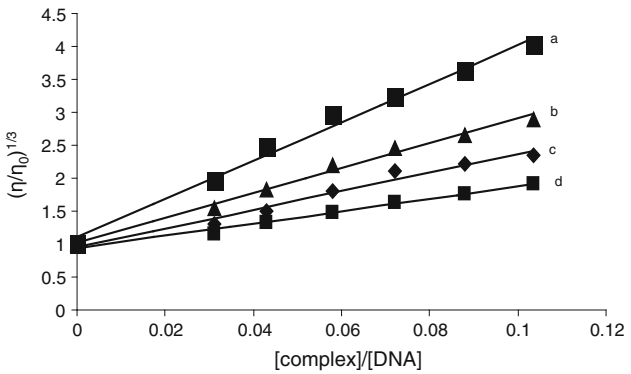

Fig. 4 Effect of increasing amount of ethidium bromide (**a**) complexes $[Co(phen)_2(2\text{-HEPIP})](ClO_4)_3$ (**b**) $[Co(bpy)_2 2\text{-HEPIP}](ClO_4)_3$ (**c**) and $[Co(dmb)_2 2\text{-HEPIP}](ClO_4)_3$ (**d**) on relative viscosity of CT-DNA at 30 ± 0.1 °C. The total concentration of DNA is 0.25 mM, [Co] = 20 μM

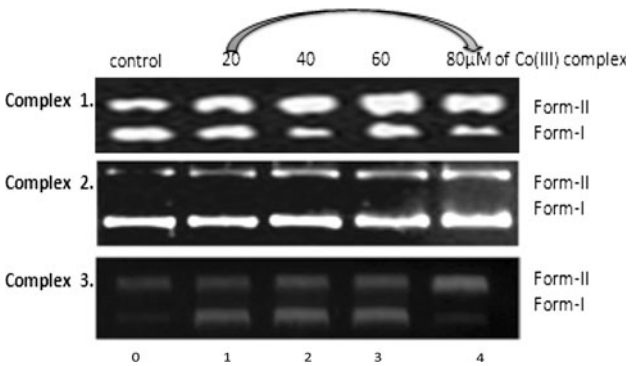

Fig. 5 Photo-activated cleavage of pBR 322 DNA in the presence of $[Co(phen)_2 2\text{-EHPIP}]^{3+}](\mathbf{1})$, $[Co(bpy)_2 2\text{-HEPIP}]^{3+}](\mathbf{2})$ and $[Co(dmb)_2 2\text{-HEPIP}]^{3+}](\mathbf{3})$complexes, after irradiation at 365 nm. Lane a control plasmid DNA (untreated pBR 322), *lanes 1–4*, addition of complexes 20, 40, 60 80 μM

Table 2 Antifungal activity of the Cobalt(III) complexes

Complex	Inhibition zone diameter (mm) of bacterial species	
	A. niger	*F. oxysporium*
$[Co(phen)_2$ 2-HEPIP$]^{3+}$ (3)	22.0 ± 0.3	20.0 ± 0.1
$[Co(bpy)_2$ 2-HEPIP$]^{3+}$ (1)	9.0 ± 0.2	11.0 ± 0.4
$[Co(dmb)_2$ 2-HEPIP$]^{3+}$ (2)	12.0 ± 0.1	11.0 ± 0.2
Fluconazole (standard)	15–18	15–18

Table 3 Antibacterial activity of the Cobalt(III) complexes

Complex	Inhibition zone diameter (mm) of bacterial species	
	S. aureus	*E. coli*
$[Co(phen)_2$ 2-HEPIP$]^{3+}$ (3)	18.0 ± 0.1	17.0 ± 0.2
$[Co(bpy)_2$ 2-HEPIP$]^{3+}$ (1)	10.0 ± 0.3	09.0 ± 0.1
$[Co(dmb)_2$ 2-HEPIP$]^{3+}$ (2)	09.0 ± 0.4	85.0 ± 0.4
Streptomycin (standard)	13–17	13–17

Values of zone of inhibition (mm, including the diameter of the disc)

Table 4 The Cytotoxic activity of the compounds

S. No	A549	DU145	HELA	HEPG2
Complex-1	23 ± 1.4	24 ± 0.8	30 ± 1.0	27 ± 1.0
Complex-2	87 ± 1.8	58 ± 0.6	> 100	>100
Complex-3	35 ± 2.3	32 ± 0.4	> 100	>100
Cisplatin	12 ± 1.0	6 ± 0.5	19 ± 1.2	7 ± 0.3

IC50 values are given in μM, and cisplatin is included for comparison. Data are presented as mean values standard deviations, and cell viability assessed after 48 h of incubation

standard drug streptomycin. Complexes **2** and **3** showed less activity against these bacteria than streptomycin. Earlier studies have given results which were also similar to this study [10, 11].

Cytotoxicity studies

The positive results obtained from the DNA-binding and cleavage experiments encouraged us to test the cytotoxicities of the complexes against a panel of human cancer cell lines, namely, human cervical cancer cell line HeLa, A549, DU145 and HEPG tumor by colorimetric (MTT) assay. The complexes were dissolved in DMSO, and blank samples containing the same volume of DMSO were taken as controls. The results were analyzed by means of cell viability and expressed as IC_{50} values as shown in Table 4. The results of the in vitro cytotoxicity studies further confirm the binding of the complexes to DNA, which consequently leads to cell death. The MTT assay was employed to measure the metabolic activity of mitochondria in the cells, based on the principle that living cells are capable of reducing the lightly colored tetrazolium salt into an intensely colored formazan derivative [46]. Figure 6 shows the viability of HeLa, A549, DU145 and HEPG cells upon treatment with complexes **1–3** for 48 h; all three complexes show only slight cytotoxicity toward HeLa, A549, DU145 and HEPG tumor cells. Complex **1** exhibits more cytotoxicity than **2** and **3**, and the complexes are less cytotoxic than the standard drug cisplatin. These results are in accordance with those reported previously for analogous cobalt polypyridyl complexes [47]. For example, the IC_{50} value of $[Co(phen)_2$ pip$]^{3+}$ is 54.6 μM L^{-1} [47].

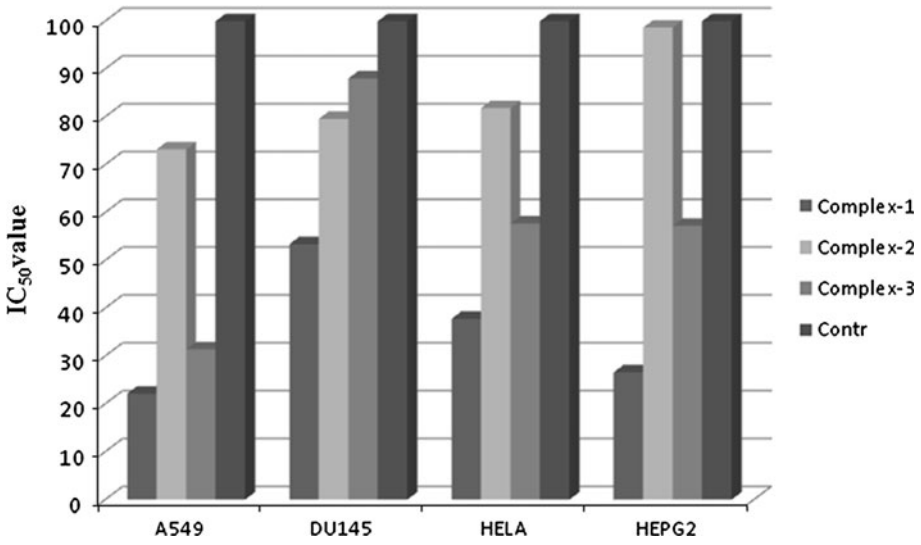

Fig. 6 In vitro cytotoxicity of complexes **1–3** on four different tumor cells. Cytotoxicity was measured by MTT reduction assay after 48 h. Untreated cells are used as the control

Molecular docking

These Co(III) complexes can interact with DNA by hydrogen bonding, particularly involving N7 of adenine, N3 of guanine, N1 of cytosine and thymine and phosphate oxygen. Also, van der Waal's attractions and π–π stacking between the complex and DNA chain is possible. Our modeling results showed that these complexes can bind to DNA with three strong hydrogen bonds, with GOLD fitness scores of 42.532 (**1**) > 30.889 (**2**) > 28.887 (**3**). Hence, the order of GOLD fitness scores from molecular docking studies matches with the spectroscopic results.

Conclusion

A new ligand HEPIP and three of its cobalt(III) complexes were prepared and characterized by elemental analysis, ESI–MS, IR and ^{1}H NMR. These complexes have high DNA-binding affinity, interacting with DNA by intercalation. Complex **1** shows the highest cytotoxicity against the four tumor cell lines. Upon irradiation at 365 nm, all three complexes can cleave plasmid DNA.

Acknowledgments We are grateful to UGC New Delhi for financial support and CFRD Osmania University for recording NMR and also grateful to Dr. Shasi Vardhan Kalivendi Senior Scientist Indian Institute of Chemical Technology (IICT), Hyderabad, for helping biological studies.

References

1. Pyle AM, Barton JK (1990) Prog Inorg Chem 38:413
2. Sigman DS, Mazumder A, Perrin DM (1993) Chem Rev 93:2295
3. Thederahn TB, Spassky A, Kuwabara MD, Sigman DS (1990) Biochem Biophys Res Commun 168:756
4. Huang HL, Li ZZ, Wang XZ, Liang ZH, Liu YJ (2012) J Coord Chem 8:3287
5. Waring MJ (1981) Ann Rev Biochem 50:159
6. Dervan PB (2001) Bioorg Med Chem 9:2215
7. Rosenberg B, Van Camp L, Trosko JE, Mansour VH (1969) Nature (London) 222:385
8. Bratsos I, Jedner S, Gianferrara T, Alessio E (2007) Met Med 61:692
9. Xie YY, Jianlin G, Jiang GB, Liang ZH, Huang HL (2013) J Coord Chem. doi:10.1007/2-11243-013-9724-6
10. Reedijik J (2009) Eur J Inorg Chem 10:1303
11. Song H, Kaiser JT, Barton JK (2012) Nat Chem 4:615–620. doi:10.1038/nchem.1375
12. Niyazi H, Hall JP, Sullivan K, Winter G, Sorensen T, Kellyand JM, Cardin CJ (2012) Nat Chem 4:62–1628. doi:10.1038/NCHEM.1397
13. Yata PK, Shilpa M, Nagababu P, Reddy MR, Reddy KL, Gabra NM, Satyanarayana S (2012) J Fluoresc 22:835
14. Vidhisha S, Reddy KL, Kumar KA, Kumar YP, Satyanarayana S (2010) Transition Met 35:1027
15. Shilpa M, Nagababu P, Latha JNL, Devi AG, Nagarjuna A, Kumar YP, Satyanarayana S (2012) J Incl Phenom Macrocycl Chem 70:187. doi:10.1007/s10847-010-9891-4
16. Devi CS, Anil KD, Singh SS, Gabra N, Deepika N, Kumar YP, Satyanarayana S (2013) Eur J Inorg Chem 64:410
17. Deepika N, Kumar YP, Devi CS, Reddy PV, Srishailam A, Satyanarayana S (2013) J Biol Inorg Chem. doi: 10.1007/s00775-013-1018-0 (article in press)
18. Srishailam A, Kumar YP, Gabra NMD, Reddy PV, Deepika N, Veerababu N, Satyanarayana S (2013) J Fluoresc. doi:10.1007/s10895-013-1209-7 (article in press)
19. Gabra NM, Mustafa B, Kumar YP, Devi CS, Shilpa M, Reddy KL, Satyanarayana S (2013) Med Chem Res. doi:10.1007/s00044-013-0617-1 (article in press)
20. Ciofini I, Lainé PP, Bedioui F, Adamo C (2004) J Am Chem Soc 126:10763
21. Tiwary AS, Mukherjee AKJ (2008) Mol Struct (Theochem) 859:107
22. Perrin DD, Annarego WLF, Perrin DR (1980) Purification of laboratory chemicals, 2nd edn. Pergamonress, New York
23. Marmur J (1961) J Mol Biol 3:208
24. Reichmann ME, Rice SA, Thomas CA, Doty P (1954) J Am Chem Soc 76:3047
25. Yamada M, Tanaka Y, Yoshimoto Y, Kuroda S, Shimo I (1992) Bull Chem Soc Jpn 65:1006
26. Vlcek AA (1967) Inorg Chem 6:1425
27. Nagababu P, Shilpa M, Latha JNL, Bhatnagar I, Srinivas PNB, Kumar YP, Reddy KL, Satyanarayana S (2011) J Fluoresc 21:563
28. Shilpa M, Nagababu P, Kumar YP, Latha JNL, Reddy MR, Karthikeyan KS, Satyanarayana S (2011) J Fluoresc 21:1155
29. Mc Ghee JD, Von Hippel PH (1974) J Mol Biol 86:469
30. Chaires JB, Dattagupta N, Crothers DM (1982) Biochemistry 21:3927
31. Satyanarayana S, Dabrowiak JC, Chaires JB (1993) Biochemistry 32:2573
32. Drew WL, Barry AL, O'Toole R, Sherris JC (1972) Appl Microbiol (Am Soc for Microbiol) 24:240
33. Tselepi-Kalouli E, Katsaros N (1989) J Inorg Biochem 37:271
34. Wolfe A, Shimer GH, Mechan T (1987) Biochemistry 26:6392
35. Tysoe SA, Morgan RJ, Baker AD, Strekas TC (1993) J Phys Chem 97:1707
36. Nair RB, Teng ES, Kirkland SL, Murphy CJ (1998) Inorg Chem 37:139
37. Moucheron C, Mesmaeker AKD, Choua C (1997) Inorg Chem 36:584
38. Chaires JB, Dattagupta N, Crothers DM (1982) Biochemistry 21:3927
39. Joseph R, Lakowicz GW (1973) Biochemistry 12:4161
40. Lakowicz JR (1983) Principles of fluorescence spectroscopy. Plenum Press, NewYork
41. Drew WL, Barry AL, O'Toole R, Sherris JC (1972) Appl Environ Microbiol 1. 97224:240
42. Satyanarayana S, Dabrowiak JC, Chaires JB (1992) Biochemistry 31:9319
43. Barton JK, Raphael AL (1984) J Am Chem Soc 106:2466
44. Sathyadevi P, Krishnamoorthy RR, Butorac AH (2012) Cowley. Metallomics, N. Dharmaraj, p 4498
45. Raja DS, Bhuvanesh SP, Natarajan K (2012) Dalton Trans 41:4365
46. Mosmann T (1983) J Immunol Methods 65:55
47. Liu J, Zou XH, Zhang QL, Mei W-J, Liu J-Z, Ji LN (2000) Met Based Drugs 76:343